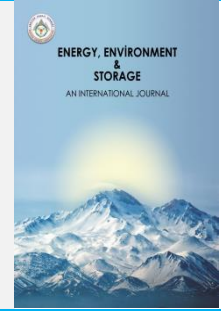




Energy, Environment and Storage

Journal Homepage: www.enenstrg.com



The Effect of Geometric Form and Spring Dynamics on Vibration Performance in Bladeless Wind Turbines with Fixed Surface Area

Mustafa Arman Özbilge¹, Berke Kirpiksiz², Mehmet Parlak³

¹Erciyes University, Faculty of Engineering, Dept. of Mech. Eng. 38280, Kayseri, Türkiye

²Erciyes University, Faculty of Engineering, Dept. of Mech. Eng. 38280, Kayseri, Türkiye

³Erciyes University, Faculty of Engineering, Dept. of Mech. Eng. 38280, Kayseri, Türkiye, ORCID: 0000-0002-3033-9887

ABSTRACT. This study experimentally investigates the effect of geometric shape and other mechanical components on vibration efficiency in bladeless wind turbines. Within the scope of the study, cylindrical and conical models with a constant surface area of 108 cm² were manufactured using a 3D printer, with PLA used for the upper surface and PETG for the lower surface. The models were tested in various configurations using a steel spring mechanism with a diameter of 2 cm, lengths of 7.5 cm, 11 cm, and 20 cm, and corresponding spring constants of 205 N/m, 140 N/m, and 77 N/m. Experiments conducted in a laboratory environment at wind speeds ranging from 4 m/s to 6.2 m/s showed that the maximum acceleration value of 5.65 m/s² was obtained for the cylindrical model with the shortest spring. The results indicate that, at low wind speeds, cylindrical geometry and higher spring stiffness provide maximum vibration intensity.

Keywords: Bladeless turbine, VIV, Acceleration analysis, 3D prototyping, Geometric comparison

Article History: Received: 23.12.2025; Revised: 28.01.2026; Accepted: 05.02.2026; Available Online: 06.02.2026

Doi: <https://doi.org/10.52924/ZSJO9405>

1. INTRODUCTION

Energy is one of the most fundamental requirements of human society. Although technological advancements have facilitated easier access to energy, the rapid growth of the global population has led to a parallel increase in energy demand, causing existing resources to become insufficient. In addition, rising and fluctuating energy costs have increased interest in more economical and sustainable energy solutions. In this context, wind energy stands out as one of the most viable renewable energy sources.

Wind energy has been used for various purposes since ancient Egyptian times, historically proving to be a reliable and efficient source of power. With technological progress, methods of harnessing wind energy have diversified and different turbine designs have been developed. However, despite their high efficiency, conventional wind turbines present significant disadvantages such as high installation and maintenance costs, large land requirements, noise generation, visual pollution, and negative impacts on bird populations. Furthermore, continuously moving mechanical components such as blades, bearings, and gears limit system lifespan and increase maintenance needs.

As an alternative to these limitations, bladeless systems utilize wind energy through a vibration-based mechanism rather than the classical rotational blade approach. These systems do not require rotating blades, bearings, or complex mechanical components during electricity generation. Their operating principle is based on the

formation of vortices around a bluff body due to flow separation, which creates periodic pressure fluctuations and induces oscillatory motion in the structure (vortex-induced vibrations). A vertically positioned cylindrical or conical body vibrates under wind influence, and the resulting mechanical oscillations are converted into electrical energy through electromagnetic or piezoelectric transducers. In this respect, these systems can be considered aeroelastic energy harvesting structures.

Previous studies have demonstrated that the energy output and vibration performance of such systems are directly dependent on aerodynamic parameters, including geometric design and surface characteristics, as well as material properties such as stiffness, density, and damping behavior. Variations in these parameters significantly affect the vortex shedding frequency, vibration amplitude, and overall energy conversion efficiency.

The increasing need to reduce dependence on fossil fuels and to develop sustainable energy solutions has led to growing interest in bladeless wind turbines. In this study, based on insights from the literature, conical and cylindrical models with equal total surface areas were fabricated using 3D printing. To ensure experimental reliability, the base structure and connection components were also designed and manufactured. While maintaining a constant total surface area of 18 × 6 cm², the effect of form factor on acceleration-based vibration performance was

*Corresponding author: mozbilge45@gmail.com

systematically investigated using RMS vibration values. [1-5]

2. MATERIALS AND METHODS

2.1 Model Design and Manufacturing

The models were manufactured using a hybrid material structure through an additive manufacturing (3D printing) process, allowing precise control over geometric dimensions and material distribution. To preserve and accurately represent the aerodynamic surface characteristics, the main body section was printed in both cylindrical and conical geometries using colored polylactic acid (PLA) filament, which offers sufficient surface smoothness and dimensional stability for experimental investigations [6].

A steel spring with a diameter of 2 cm was employed as the mechanical transmission and elastic element between the vibrating body and the fixed base. This spring enabled controlled oscillatory motion by providing the necessary restoring force and flexibility, while also facilitating efficient transfer of vibration energy. The selection of steel as the spring material ensured consistent stiffness and durability under repeated dynamic loading conditions.

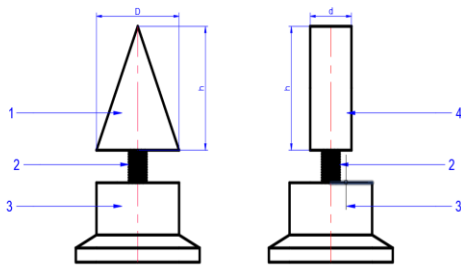


Fig. 1. Schematic drawings of the system. (1- conical part ($D = 12$ cm, $h = 18$ cm) 2- 7.5 cm, 11 cm, 20 cm springs, 3- Support part, 4- Cylindrical part ($d = 6$ cm, $h = 18$ cm))

Figure 1 shows schematic drawings of investigated models. In this figure, there are two models; 1- conical model and 2- cylindrical model. Both models have the same wind-catching surface area. The lower base was manufactured from blue polyethylene terephthalate glycol (PETG) material to enhance structural robustness and resistance to cyclic and dynamic loads during testing. PETG was preferred due to its higher impact strength and toughness compared to PLA, thereby minimizing deformation and ensuring stable boundary conditions throughout the experimental process. This hybrid material approach allowed the mechanical and aerodynamic components of the system to be optimized independently, contributing to repeatable and reliable vibration performance measurements. [7] Figure 2 illustrates models of fabricated using 3D printing.

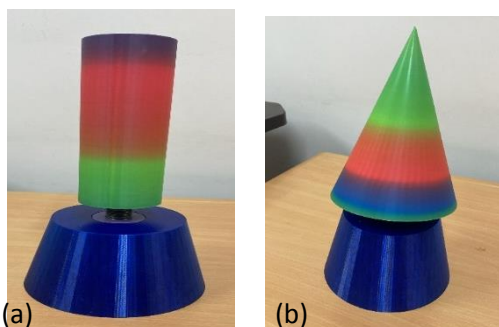


Fig.2 (a) A conical bladeless (b) A cylindrical bladeless of wind turbine was fabricated using 3D printing

2.2 Experimental Setup and Data Acquisition

The experiments were conducted in the Motors Laboratory using a controlled axial fan. In the initial stage, the component manufactured from PETG polymer for the lower base was positioned in front of the fan at a location providing maximum aerodynamic efficiency. Subsequently, to improve the accuracy of the measurements obtained from the PLA components, the contact surfaces where the vibration measurement system would be mounted were smoothed by sanding to ensure proper alignment. After completing the necessary preparations, the fan was activated. For safety reasons, the fan operating frequency was limited to a maximum of 45 Hz. Wind speed was accurately determined using anemometer sensors placed in front of the fan, and measurements were recorded at wind velocities of 4 m/s, 5.8 m/s, and 6.2 m/s. Vibration measurements were then performed using three different spring configurations. All measurements were conducted under appropriate supervision. In this experimental study, wind speed and geometric configuration were considered as the primary independent variables [8]. Figure 3 shows experimental setup.

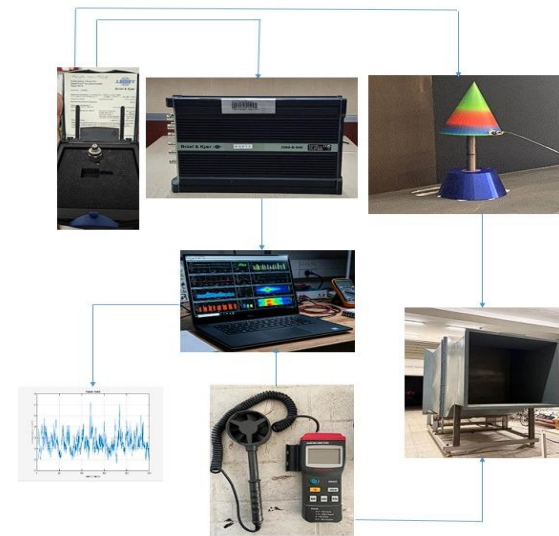


Fig. 3. Experimental setup and working diagram

3. RESULTS AND DISCUSSION

The acceleration data obtained from the experiments reveal the vibration intensity, which represents the energy generation potential of the turbine. In this study, vibration analysis was conducted to reveal the dynamic behaviour of the bladeless wind turbine. The Root Mean Square (RMS) value, widely used in vibration measurements, is considered a fundamental parameter for determining the overall vibration level of the system, as it represents the energy content of the vibration. However, evaluating only the RMS magnitude is not sufficient to fully understand the dynamic characteristics of the system. Vibration signals with identical RMS values may possess different frequency contents. Therefore, accurate interpretation of vortex-induced vibrations in bladeless wind turbines requires that RMS values be analyzed together with their frequency

components. RMS and velocity values and RMS and Frequency values for each materials for each materials are given in table 1 and table 2., respectively.

Table 1 : RMS and Velocity Values For Each Materials

Material	Spring Type	Velocity m/s	Approx. RMS Value m/s^2
Conical	Short	4	0.80
Conical	Medium	4	0.85
Conical	Long	4	0.22
Cylindrical	Short	4	1.95
Cylindrical	Medium	4	1.70
Cylindrical	Long	4	0.28
Conical	Short	5.8	0.70
Conical	Medium	5.8	0.38
Conical	Long	5.8	0.28
Cylindrical	Short	5.8	1.85
Cylindrical	Medium	5.8	2.35
Cylindrical	Long	5.8	0.85
Conical	Short	6.2	0.75
Conical	Medium	6.2	0.52
Conical	Long	6.2	0.32
Cylindrical	Short	6.2	1.5
Cylindrical	Medium	6.2	2.55
Cylindrical	Long	6.2	1.20

Table 2 : RMS and Frequency Values For Each Materials

Material	Spring type	Approx. RMS Value m/s^2	Frequency (Hz)
Conical	Short	0.80	0.0318
Conical	Medium	0.85	0.0338
Conical	Long	0.22	0.0088
Cylindrical	Short	1.95	0.0776
Cylindrical	Medium	1.70	0.0677
Cylindrical	Long	0.28	0.0111
Conical	Short	0.70	0.0192
Conical	Medium	0.38	0.0104
Conical	Long	0.28	0.0077
Cylindrical	Short	1.85	0.0508
Cylindrical	Medium	2.35	0.0645
Cylindrical	Long	0.85	0.0233
Conical	Short	0.75	0.0193
Conical	Medium	0.52	0.0133
Conical	Long	0.32	0.0082
Cylindrical	Short	1.5	0.0385
Cylindrical	Medium	2.55	0.0655
Cylindrical	Long	1.20	0.0308

Fig.4. Acceleration step graph of shortest (a), medium (b) and (c) long spring that is subjected to vibration at a speed of 4 meters per second (Conical)

Vortex shedding occurs within a specific frequency range, and when this frequency interacts with the natural frequency of the structure, the vibration amplitude can increase significantly. This interaction directly affects the energy harvesting potential of the system. In this context, the effective vibration acceleration parameter, *a*_{RMS}, was evaluated together with frequency analysis [9-12]. Figure 5-6 shows acceleration step values for conical model and 4, 5.8 and 6.2 m/s

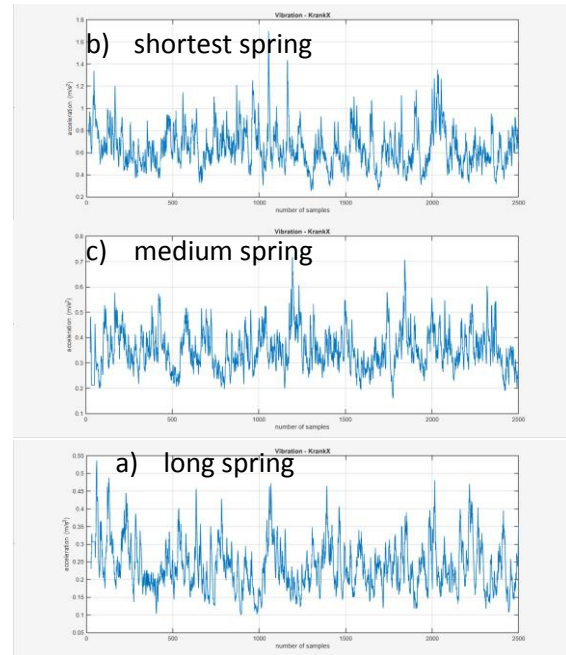


Fig.5. Acceleration step graph of shortest (a), medium (b) and (c) long spring that is subjected to vibration at a speed of 5.8 meters per second (Conical)

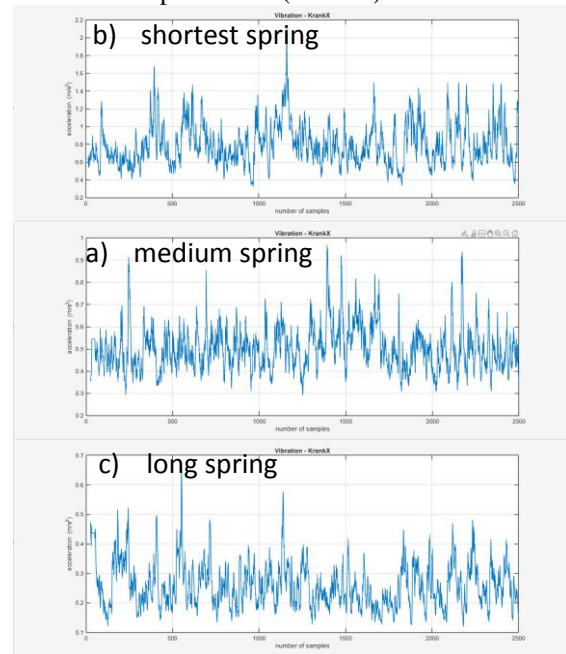


Fig.6. Acceleration step graph of shortest (a), medium (b) and (c) long spring that is subjected to vibration at a speed of 6.2 meters per second (Conical)

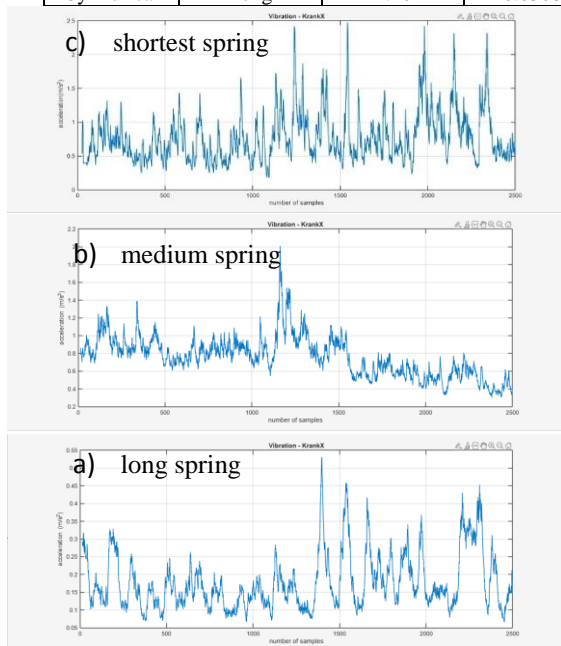


Figure 7,8 and 9 shows acceleration step values for cylindrical model and 4, 5.8 and 6.2 m/s.

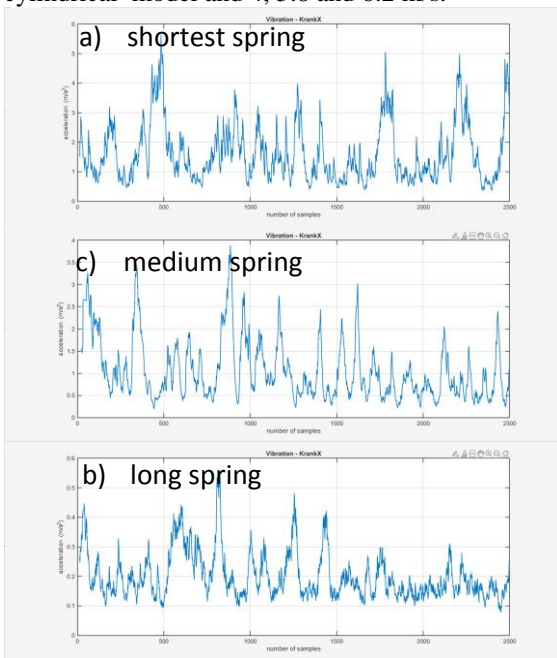


Fig.7. Acceleration step graph of shortest (a), medium (b) and (c) long spring that is subjected to vibration at a speed of 4 meters per second (cylindrical)

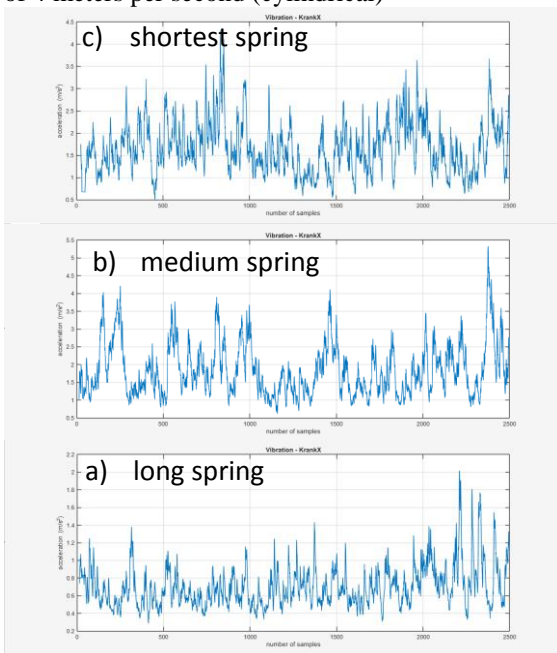


Fig. 8. Acceleration step graph of long spring that is subjected to vibration at a speed of 5.8 meters per second. . (Cylindrical)

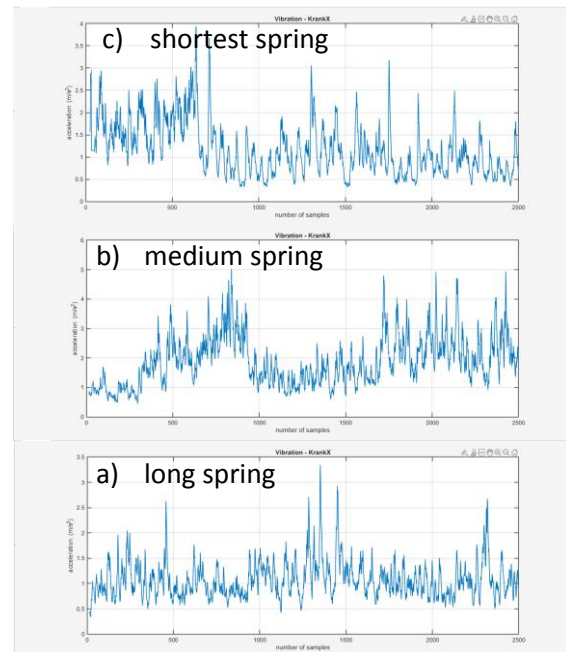


Fig. 9. Acceleration step graph of long spring that is subjected to vibration at a speed of 6.2 meters per second. . (Cylindrical)

4. CONCLUSION

4.1 Comparative Analysis of Vibrational Response

The experimental results summarized in Table 1 demonstrate a clear correlation between flow velocity (m/s) and the resulting Root Mean Square (RMS) acceleration (m/s²) for the tested geometric configurations. Under identical flow velocities and spring conditions, cylindrical structures consistently produce markedly higher RMS values than their conical counterparts. For example, at a velocity of 6.2 m/s, the cylindrical structure fitted with a medium spring attained an RMS value of 2.55 m/s², whereas the conical structure under the same conditions generated only 0.52 m/s².

The relationship between vibration intensity and oscillation frequency (Hz), presented in Table 2, further supports the enhanced dynamic response of the cylindrical geometry. Elevated RMS values are closely associated with increased oscillation frequencies. At 4 m/s, the cylindrical-short configuration reached a frequency of 0.0776 Hz with an RMS of 1.95 m/s², while the conical-short configuration at the same velocity exhibited a substantially lower frequency of 0.0318 Hz.

4.2 Efficiency and Optimal Configurations

From a mechanical efficiency perspective—defined here as the capacity of the structure to transform fluid kinetic energy into structural vibration—the Cylindrical-Medium and Cylindrical-Short configurations provide the most effective performance. The highest performance level was observed for the cylindrical structure with a medium spring at 6.2 m/s, where the maximum RMS value of 2.55 m/s² and a frequency of 0.0655 Hz were recorded. In contrast, conical structures, particularly those employing long springs, exhibited the lowest efficiency, with RMS values decreasing to as little as 0.22 m/s².

4.3 Implications of Maintaining Constant Surface Area

The choice to preserve a constant surface area for both cylindrical and conical geometries constitutes a crucial

control parameter in this investigation. This decision introduces both analytical strengths and limitations:

4.3.1 Advantages

- It ensures that differences in vibrational behavior arise primarily from geometric form and fluid-structure interaction rather than disparities in flow exposure area.
- It enables a normalized assessment of energy capture per unit area, demonstrating that cylindrical geometries are more susceptible to synchronize vortex shedding compared to conical forms.

4.3.2 Disadvantages

- For conical geometries, maintaining a constant surface area necessitates adjustments between base diameter and height. This constraint can introduce *frequency dispersion*, where varying local diameters promote vortex shedding at different frequencies along the structure, thereby reducing the overall RMS response.
- Cylindrical geometries benefit from a uniform diameter, which facilitates global synchronization of vortex-induced vibrations (VIV). This advantage is inherently restricted in conical designs under a fixed surface area constraint.

Finally, the cylindrical geometry—particularly when combined with short or medium elastic supports—demonstrates a more stable and efficient dynamic response in flow-induced vibration applications than the conical geometry. These results are consistent with reference [13].

REFERENCES

- [1] E. Akköse, O. Ö. Mengi, ve K. Yanmaz “Kanatsız Rüzgar Türbini Tasarımı,” *Karadeniz Fen Bilimleri Dergisi*, c. 8, s. 56–69, 2018, doi:10.31466/kfbd.425547
- [2] Bahadır, I. . Dynamic Modeling and Investigation of a Tunable Vortex Bladeless Wind Turbine. *Energies*, **15**(18), 6773., 2022, <https://doi.org/10.3390/en15186773>
- [3] Kang, H., Kook, J., Lee, J., & Kim, Y.-K., A Novel Small-Scale Bladeless Wind Turbine Using Vortex-Induced Vibration and a Discrete Resonance-Shifting Module. *Applied Sciences*, **14**(18), 8217. , 2024, <https://doi.org/10.3390/app14188217>
- [4] T.-Z. Ang, M. Salem, M. Kamarol, H. S. Das, M. A. Nazari, and N. Prabaharan, “A comprehensive study of renewable energy sources: Classifications, challenges and suggestions,” *Energy Strategy Reviews*, vol. 43, p. 100939, Sep. 2022, <https://doi.org/10.1016/j.esr.2022.100939>
- [5] F. Soyduğan, *Rüzgâr Enerjisi, Bilim ve Teknik*, Kasım. (PDF) ,2021 <https://bilimteknik.tubitak.gov.tr/wp-content/uploads/sites/154/2025/09/7803c8bf-c661-4d68-b77c-4cbcb6471cbe-1.pdf>
- [6] Martins, R. F., Branco, R., Martins, M., Macek, W., Marciniak, Z., Silva, R., Trindade, D., Moura, C., Franco, M., & Malça, C. . Mechanical properties of additively manufactured PLA and PETG. *Polymers*, **16**(13), 2024, <https://doi.org/10.3390/polym16131868>
- [7] Budziński, B., & Federowicz, K., Evaluation of PLA and PETG as 3D-printed reference materials for compressive strength testing. *Materials*, **18**(16), 3794, 2025, <https://doi.org/10.3390/ma18163794>
- [8] Mohamed, Z., Soliman, M., Feteha, M. et al. A novel optimal design approach for bladeless wind turbines considering mechanical properties of composite materials used. *Sci Rep* **15**, 1355 (2025). <https://doi.org/10.1038/s41598-024-82385-9>
- [9] Artigao, E., Koukoura, S., Honrubia-Escribano, A., Carroll, J., McDonald, A., Gómez-Lázaro, E., Current Signature and Vibration Analyses to Diagnose an In-Service Wind Turbine Drive Train. *Energies*, **11**(4), 960 , 2018, <https://doi.org/10.3390/en11040960>
- [10] Kowalska-Koczwara, A., Rizzo, F., Sabbà, M. F., & Bedon, C. , Assessing the Influence of RMS and VDV on Analysis of Human Perception of Vibrations in Buildings Caused by Selected Sources of Traffic. *Applied Sciences*, **14**(9), 3688., 2024, <https://doi.org/10.3390/app14093688>
- [11] Erdiwansyah, Mahidin, Husin, H. et al., A critical review of the integration of renewable energy sources with various technologies. *Prot Control Mod Power Syst* **6**, 3 (2021). <https://doi.org/10.1186/s41601-021-00181-3>
- [12] Pavan Kumar, B. K., & Basavaraj, Y., Vibration analysis of frequency domain data using MATLAB for application of rotating part machines in industry. *SSRG International Journal of Mechanical Engineering* **10** (1), 1-15, 2023, <https://doi.org/10.14445/23488360/IJME-V10I1P101>
- [13] Ma, L., Li, Z., Yang, S., & Wang, J.,. A review on vibration sensor: Key parameters, fundamental principles, and recent progress on industrial monitoring applications. *Vibration*, **8**(4), 56., 2025, <https://doi.org/10.3390/vibration8040056>